Neurochemical Research (2019) 44:796–810
https://doi.org/10.1007/s11064-018-02713-0

ORIGINAL PAPER

Long-term Therapeutic Effects of Extracorporeal Shock Wave-Assisted Melatonin Therapy on Mononeuropathic Pain in Rats

Chien-Hui Yang[1] · Hon-Kan Yip[2,3,4,5,6] · Hung-Fei Chen[7] · Tsung-Cheng Yin[8] · John Y. Chiang[9] · Pei-Hsun Sung[2] · Kun-Chen Lin[1] · Yu-Huan Tsou[1] · Yi-Ling Chen[2] · Yi-Chen Li[2] · Tien-Hung Huang[2] · Chi-Ruei Huang[2] · Chi-Wen Luo[2] · Kuan-Hung Chen[1,4]

Received: 6 August 2018 / Accepted: 31 December 2018 / Published online: 10 January 2019

Abstract

We evaluated the ability of extracorporeal shock wave (ECSW)-assisted melatonin (Mel) therapy to offer an additional benefit for alleviating the neuropathic pain (NP) in rats. Left sciatic nerve was subjected to chronic constriction injury (CCI) to induce NP. Animals (n = 30) were randomized into group 1 (sham-operated control), group 2 (CCI only), group 3 (CCI + ECSW), group 4 (CCI + Mel) and group 5 (CCI + ECSW + Mel). By days 15, 22 and 29 after CCI, the thermal paw withdrawal latency (TPWL) and mechanical paw withdrawal threshold (MPWT) were highest in group 1, lowest in group 2, significantly higher in group 5 than in groups 3 and 4, but they showed no difference between the later two groups (all $p < 0.0001$). The protein expressions of inflammatory (TNF-α, NF-κB, MMP-9, IL-1ß), oxidative-stress (NOXs-1, -2, -4, oxidized protein), apoptotic (cleaved-caspase3, cleaved-PARP), DNA/mitochondrial-damaged (γ-H2AX/cytosolic-cytochrome C), microglia/astrocyte activation (ox42/GFAP), and MAPKs [phosphorylated (p)-p38, p-JNK, p-ERK] biomarkers in dorsal root ganglia neurons (DRGs) and in spinal dorsal horn were exhibited an opposite pattern of TPWL among the five groups (all $p < 0.0001$). Additionally, protein expressions of Nav.1.3, Nav.1.8 and Nav.1.9 in sciatic nerve exhibited an identical pattern to inflammation among the five groups (all $p < 0.0001$). The numbers of cellular expressions of MAPKs (p-ERK1/2+/peripherin + cells, p-ERK1/2+/NF200 + cells and p-JNK+/peripherin + cells, p-JNK+/NF200 + cells) and voltage-gated sodium channels (Nav.1.8+/peripherin + cells, Nav.1.8+/NF200 + cells, Nav.1.9+/peripherin + cells, Nav.1.9+/NF200 + cells) in small and large DRGs displayed an identical pattern to inflammation among the five groups (all $p < 0.0001$). In conclusion, the synergistic effect of combined ECSW-Mel therapy is superior to either one alone for long-term improvement of mononeuropathic pain-induced by CCI in rats.

Keywords Behavior test · Dorsal root ganglion · Spinal dorsal horn · Protein kinase · Inflammation · Oxidative stress

Introduction

The processes of cellular apoptosis, DNA and mitochondrial damage, oxidative stress, neuro-inflammation, inflammatory cells and cytokines production have been revealed to be the major molecular-cellular perturbations of neuropathic pain (NP) [1–5] that may account for why the traditional pharmaceuticals and non-pharmaceuticals therapy [6, 7] is frequently failed to cure. These aforementioned issues raise a concern that single therapeutic option may not be enough for achieving the therapeutic purpose in alleviating the NP. To solve the problem, the present mission is to develop a novel combination therapy with different therapeutic mechanisms and long-term duration of effectiveness.

N-acetyl-5-methoxytryptamine (melatonin), an indole hormone mainly derived from the mitochondria of pineal gland that has been identified to have a broad range of biological functions, especially acts as free radical scavenger [8]. While melatonin was originally recognized as an endogenous molecule specializing in the modulation of circadian pattern in mammals, it is later identified to have capacities of pain modulation, anti-inflammation and immunomodulation as well as acts on suppressing the generation of oxidative

Chien-Hui Yang and Hon-Kan Yip have contributed equally and share first authorship.

✉ Kuan-Hung Chen
amigofx35@gmail.com

Extended author information available on the last page of the article

stress [9, 10]. On the other hand, extracorporeal shock wave (ECSW) had been originally proved as a useful therapeutic modality for the disintegration of body calculi [11]. Its current utilizations are mainly in soft tissue/muscle-skeletal pain relief [12] and wound, tendon and bone healing [13, 14] as well as in ischemic organ dysfunction [10, 15]. The underlying mechanisms of ECSW therapy involving in improvement of the aforementioned disorders have been identified to be multifactorial such as anti-inflammation, anti-oxidation, neuro-protective effect and angiogenesis.

Interestingly, studies have previously demonstrated that members of mitogen activated protein kinases (MAPKs) such as p38, ERK, and JNK (i.e., MAPK family), have all involved in the propagation and maintenance of chronic pain in both dorsal root ganglion (DRG) and spinal dorsal horn (SDH) neurons [16]. Additionally, abundant evidences have pinpointed that the voltage-gated sodium channels play a critical role in pain transmission and sensitization in peripheral and central nervous system [17].

Following initiation of NP, spontaneous neuro-electrical activity of sensory input fiber is upregulated mainly through a reduction in the firing threshold and further modified by remodeling of sodium channel conductance which in turn, are changed by alternations in sodium channel gene expression and sodium channel trafficking, or phosphorylation of sodium channel proteins [18]. Amongst the family of voltage-gated sodium channels, Nav. 1.3, Nav. 1.7, Nav. 1.8 and Nav. 1.9 have been displayed to closely link to NP. Additionally, their alterations in the expression, kinetics, and distribution have been also well-documented by previous studies [18–20].

Considering NP as a refractory disorder seeking efficacious treatment, this experimental research examined the hypothesis that combined treatment involving ECSW and melatonin might be superior to either one alone for the long-term therapeutic effects on improving painful disorder and molecular-cellular perturbation in a rat model of NP. Additionally, the MAPK family and voltage-gated sodium channels were also investigated for delineating the pain-conducted pathways, i.e., signaling pathway in the setting of NP.

Materials and Methods

Ethics

All animal experimental procedures were approved by the Institute of Animal Care and Use Committee at Kaohsiung Chang Gung Memorial Hospital (Affidavit of Approval of Animal Use Protocol No. 2015051303) and performed in accordance with the Guide for the Care and Use of Laboratory Animals [The Eighth Edition of the Guide for the Care and Use of Laboratory Animals (NRC 2011)].

Animals were housed in an Association for Assessment and Accreditation of Laboratory Animal Care International (AAALAC)-approved animal facility in our hospital with controlled temperature and light cycle (24 °C and 12/12 light cycle).

Animal Model of Neuropathic Pain

Mononeuropathy was induced by performing chronic constriction injury (CCI) model on the left sciatic nerve of animals as previously described [21] and our recent report [1]. Under inhalation of 2.0% isoflurane anesthesia, the sciatic nerve of the animal was exposed after incision of the skin. Four of 4–0-gauge chromic gut wire tied around the nerve at interval of 1 mm, and the ligatures were tied loosely enough so that, under microscope inspection, the epineural blood circulation would not be obstructed. Finally, the incision was closed in layers and animals were placed in a warm condition until recovery. Sham surgery was done by exposing sciatic nerve without performing ligation.

Animal Grouping and Treatment Strategies

Pathogen-free, adult male Sprague–Dawley (SD) rats (n = 30) weighing 325–350 g (Charles River Technology, BioLASCO Taiwan Co. Ltd., Taiwan) were randomly divided into five groups: group 1 [sham-operated control (SC), i.e., the skin and muscle were opened and the sciatic nerve was exposed only without ligatures, followed by closure of the skin and muscle layers], group 2 (CCI only, i.e., induced by performing CCI procedure only), group 3 [CCI + ECSW (by applying 200 impulses/time at post-CCI 3 h and at days 3 and 7 over skin surface just at the level of femoral areas with an energy of 0.12 mJ/mm^2, respectively)], group 4 [CCI + melatonin 50 mg/kg (1 ml/kg) at 3 h after CCI procedure, followed by 20 mg/kg (0.4 ml/kg) at 18 h and 48 h after CCI procedure by intra-peritoneal administration, respectively], and group 5 (CCI + ECSW + melatonin).

The ECSW energy and melatonin dosages for the treatment of the CCI-induced neuropathic pain were based on our recent reports [1, 2, 10] with minimal modification.

Behavioral Assessments

The procedure and protocol have been described in our recent report [1]. In details, to demonstrate the significance of ECSW-melatonin therapy on attenuating neuropathic pain at chronic stages, thermal and mechanical nociceptive thresholds were measured before CCI as well as post-CCI days 15, 22, and 29. To assess for thermal hyperalgesia, the animals in each group were identically placed on a glass plate and a radiant heat (Plantar Test Apparatus; Ugo Basile, Italy) was applied to the plantar surface of the operated hind

paw. The withdrawal latency (i.e., defined the time interval of withdraw from the heat stimulus) as was recorded, with a minimal value set at 0.1 s and a maximum value (cut-off latency) set at 30 s to avoid paw injury. Each rat was tested three times at an interval of 5 min, and the mean value was employed in the analysis. On the other hand, to assess mechanical allodynia, the animal was placed in a chamber and a servo-controlled mechanical stimulus (Dynamic Plantar Aesthesiometer; Ugo Basile, Italy) was applied to the plantar surface of the operated hind paw repeatedly at 5-min interval with increasing punctate pressure until the rat withdrew its paw. A maximal cut-off value was set to 50 g to prevent tissue damage. The threshold was tested three times for each time point and the mean values were used in the analysis.

Western Blot Analysis

The ipsilateral sciatic nerve, L4–L5 dorsal root ganglia (DRGs) and corresponding dorsal horn of the spinal cord from the rats of the sham control and experimental groups were harvested as our recent report [1]. Equal amounts (50 μg) of protein extracts were loaded and separated by SDS–PAGE using 8–12% acrylamide gradients. After electrophoresis, the separated proteins were transferred electrophoretically to a polyvinylidene difluoride (PVDF) membrane (Amersham Biosciences). Nonspecific sites were blocked by incubation of the membrane in blocking buffer [5% nonfat dry milk in T-TBS (TBS containing 0.05% Tween 20)] overnight. The membranes were incubated with the indicated primary antibodies [cleaved caspase 3 (1:1000, Cell Signaling), cleaved poly (ADP-ribose) polymerase (PARP) (1:1000, Cell Signaling), cytosolic cytochrome C (1:2000, Millipore), NADPH oxidase (NOX)-1 (1:2000, Sigma), NOX-2 (1:750, Sigma), NOX-4 (1:1000, Abcam), interleukin (IL)-1β (1:1000, Cell Signaling), tumor necrosis factor (TNF)-α (1:1000, Cell Signaling), nuclear factor (NF)-κB (1:600, Abcam), matrix metalloproteinase (MMP)-9 (1:3000, Abcam), phosphorylated histone H2AX (γ-H2AX) (1/1000, Abcam), phosphorylated (p)-p38 (1:1000, Cell Signaling), p-JNK (1:1000, Abcam), p-ERK1/2 (1:1000, Abcam), Nav 1.3 (1:200, Alomone Labs), Nav 1.8 (1:2000, Abcam), Nav 1.9 (1:200, Alomone Labs), glial fibrillary acidic protein (GFAP) (1:500, DAKO) and actin (1:10,000, Millipore)] for 1 h at room temperature. Horseradish peroxidase-conjugated anti-rabbit immunoglobulin IgG (1:2000, Cell Signaling) was used as the secondary antibody for 1 h incubation at room temperature. The washing procedure was repeated eight times within an hour, and immunoreactive bands were visualized by enhanced chemiluminescence (ECL; Amersham Biosciences) after exposure to Biomax L film (Kodak). For quantification, ECL signals were digitized using Labwork software (UVP).

Immunofluorescent (IF) Staining

Immunofluorescent staining proceeded as our previously reported [1]. Rehydrated paraffin sections were first treated with 3% H_2O_2 for 30 min and incubated with Immuno-Block reagent (BioSB, Santa Barbara, CA, USA) for 30 min at room temperature. Sections were then incubated with primary antibodies specifically against p-p38 (1:500, Gene Tex), NF-200 (7.5μ g, Abcam), and peripherin (1:1000, Abcam). Sections incubated with irrelevant antibodies served as controls. Three sections of DRG specimens were analysed in each rat. For quantification, three randomly selected high-power fields (HPFs) were analysed per section. The mean number of positively-stained cells per HPF for each animal was determined across all nine HPFs.

Assessment of Oxidative Stress

The procedure and protocol for assessing the protein expression of oxidative stress have been detailed in our previous reports [1, 10]. The Oxyblot Oxidized Protein Detection Kit was purchased from Chemicon, Billerica, MA, USA (S7150). DNPH derivatization was carried out on 6 μg of protein for 15 min according to the manufacturer's instructions. One-dimensional electrophoresis was carried out on 12% SDS/polyacrylamide gel after DNPH derivatization. Proteins were transferred to nitrocellulose membranes which were then incubated in the primary antibody solution (anti-DNP 1:150) for 2 h, followed by incubation in secondary antibody solution (1:300) for 1 h at room temperature. The washing procedure was repeated eight times within 40 min. Immunoreactive bands were visualized by enhanced chemiluminescence (ECL; Amersham Biosciences, Amersham, UK) which was then exposed to Biomax L film (Kodak, Rochester, NY, USA). For quantification, ECL signals were digitized using Labwork software (UVP, Waltham, MA, USA). For Oxyblot protein analysis, a standard control was loaded on each gel.

Statistical Analysis

Quantitative data are expressed as mean ± SD. Statistical analysis was performed by ANOVA, followed by Bonferroni multiple-comparison post hoc test. Statistical analysis was also performed using SPSS (SPSS for Windows, version 13; SPSS, IL, USA). The threshold for statistical significance was considered $p < 0.05$.

Results

Mechanical Paw Withdrawal Threshold (MPWT) and Thermal Paw Withdrawal Latency (TPWL) at Days 15, 22, and 29 After CCI (Fig. 1)

By days 15, 22, 29 after CCI procedure, MPWT was highest in SC, lowest in CCI, significantly higher in CCI + ECSW + Mel than in CCI + ECSW and CCI + Mel, but it showed no difference between CCI + ECSW and CCI + Mel.

By days 15, 22, 29 after CCI procedure, TPWL was highest in SC, lowest in CCI, significantly lower in CCI + ECSW and CCI + Mel than in CCI + ECSW + Mel, and significantly lower in CCI + Mel than in CCI + ECSW. These findings suggested that combined therapy was superior to either one alone for attenuating mechanical allodynia and thermal hyperalgesia.

The Protein Expressions of Sciatic Nerve- and L4-5 DRGs-Voltage-Gated Sodium Channels by Day 30 After CCI (Fig. 2)

The protein expressions of Nav.1.3, Nav.1.8 and Nav.1.9, three indicators of voltage-gated sodium channels in sciatic nerve and L4-5 DRGs, were lowest in SC, highest in CCI, significantly higher in CCI + ECSW and CCI + Mel than in CCI + ECSW + Mel, and significantly higher in CCI + Mel than in CCI + ECSW.

The Protein Expressions of Inflammatory and Oxidative Stress Biomarkers in L4-5 DRGs by Day 30 After CCI (Fig. 3)

The protein expressions of TNF-α, NF-κB, MMP-9 and IL-1ß, four inflammatory mediators, were highest in CCI, lowest in SC, significantly higher in CCI + ECSW and CCI + Mel than in CCI + ECSW + Mel, and significantly higher in CCI + Mel than in CCI + ECSW. The protein expressions of NOX-1, NOX-2, NOX-4 and oxidized protein, four indices of oxidative stress, exhibited an identical pattern of inflammation among the five groups.

Protein Expressions of Apoptotic, Mitochondrial-Damaged and DNA Damaged Biomarkers, and Signaling Transduction Molecules in L4-5 DRGs by Day 30 After CCI (Fig. 4)

The protein expression of cleaved caspase 3 and cleaved PARP, two indicators of apoptosis, were highest in CCI, lowest in SC, significantly higher in CCI + ECSW and CCI + Mel than in CCI + ECSW + Mel, and significantly higher in CCI + Mel than in CCI + ECSW. Additionally, the protein expressions of γ-H2AX, an indicator of DNA damage, and cytosolic cytochrome C, an indicator of mitochondrial-damage, exhibited an identical pattern to apoptosis among the five groups. On the other hand, the protein expressions of phosphorylated (p)-p38, p-JNK, p-ERK1/2, three indicators of mitogen-activated protein kinases (MAPKs) for response to stress stimulations and

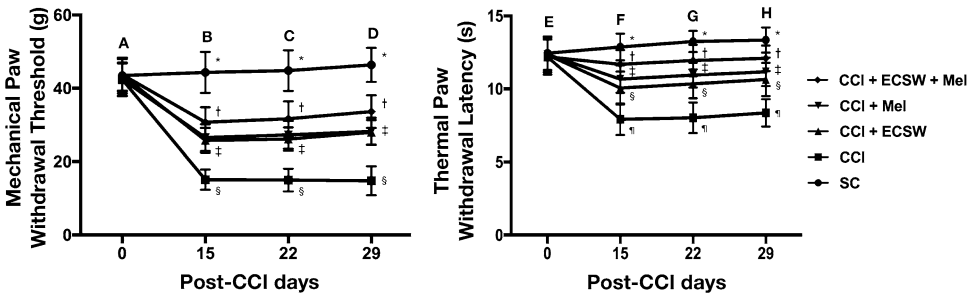

Fig. 1 ECSW-Mel therapy improved MPWT and TPWL at days 0, 15, 22 and 29 after CCI. Left: (A) By day 0, the statistical results of MPWT did not differ among the five groups. (B) day 15, the statistical results of MPWT, * denotes statistical significance versus other groups with different symbols (†, ‡, §), $p < 0.0001$. The symbol ‡ indicated CCI + ECSW and CCI + ECSW + Mel groups. (C) By day 22, the statistical results of MPWT, * denotes statistical significance versus other groups with different symbols (†, ‡, §), $p < 0.0001$. The symbol ‡ indicated CCI + ECSW and CCI + ECSW + Mel groups. (D) By day 29, the statistical results of MPWT, * denotes statistical significance versus other groups with different symbols (†, ‡, §), $p < 0.0001$. The symbol ‡ indicated CCI + ECSW and CCI + ECSW + Mel groups. Right: (E) By day 0, the statistical results of TPWL did not differ among the five groups. (F) By day 15, the statistical results of TPWL, * denotes statistical significance versus other groups with different symbols (†, ‡, §, ¶), $p < 0.0001$. (G) By day 22, the statistical results of TPWL, * denotes statistical significance versus other groups with different symbols (†, ‡, §, ¶), $p < 0.0001$. (H) By day 29, the statistical results of TPWL, * denotes statistical significance versus other groups with different symbols (†, ‡, §, ¶), $p < 0.0001$. All statistical analyses were performed by one-way ANOVA, followed by Bonferroni multiple comparison post hoc test ($n = 6$ for each group). Symbols (*, †, ‡, §) indicate significance (at 0.05 level). *MPWP* Mechanical paw withdrawal threshold, *TPWL* thermal paw withdrawal latency, *SC* sham control, *CCI* chronic constriction injury, *ECSW* extracorporeal shock wave, *Mel* melatonin

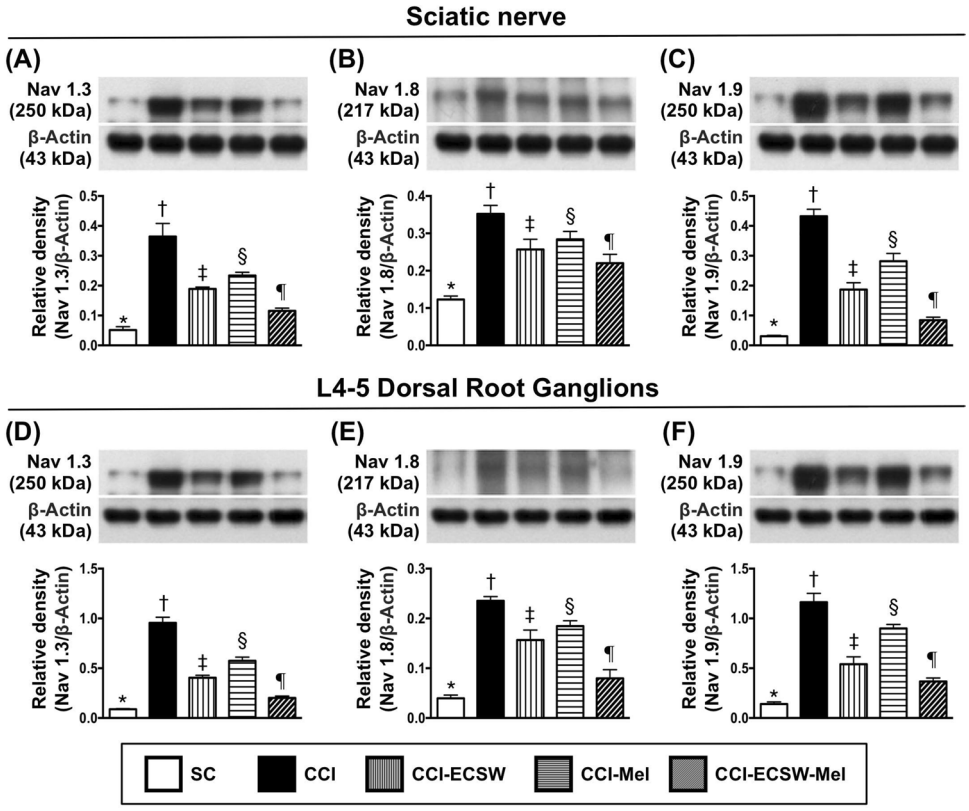

Fig. 2 The protein expressions of sciatic nerve- and L4-5 DRGs-voltage-gated sodium channels by day 30 after CCI. **a** Protein expression of Nav.1.3 in sciatic nerve, * denotes statistical significance versus other groups with different symbols (†, ‡, §, ¶), $p<0.0001$. **b** Protein expression of Nav.1.8 in sciatic nerve, * denotes statistical significance versus other groups with different symbols (†, ‡, §, ¶), $p<0.001$. **c** Protein expression of Nav.1.9 in sciatic nerve, * denotes statistical significance versus other groups with different symbols (†, ‡, §, ¶), $p<0.0001$. **d** Protein expression of Nav.1.3 in L4-5 DRGs, * denotes statistical significance versus other groups with different symbols (†, ‡, §, ¶), $p<0.0001$. **e** Protein expression of Nav.1.8 in L4-5 DRGs, * denotes statistical significance versus other groups with different symbols (†, ‡, §, ¶), $p<0.0001$. **f** Protein expression of Nav.1.9 in L4-5 DRGs, * denotes statistical significance versus other groups with different symbols (†, ‡, §, ¶), $p<0.0001$. All statistical analyses were performed by one-way ANOVA, followed by Bonferroni multiple comparison post hoc test ($n=6$ for each group). Symbols (*, †, ‡, §, ¶) indicate significance at the 0.05 level (i.e., SC vs. CCI, $p<0.0001$; CCI vs. CCI + ECSW vs. CCI + Mel vs. CCI + ECSW + Mel, $p<0.0001$; CCI + ECSW + Mel vs. CCI + ECSW, $p<0.01$; CCI + ECSW + Mel vs. CCI + Mel, $p<0.001$; CCI + ECSW vs. CCI + Mel, $p<0.05$). *SC* sham control, *CCI* chronic constriction injury, *ECSW* extracorporeal shock wave, *Mel* melatonin

pain modulation, displayed an opposite pattern to apoptosis among the five groups.

Protein Expressions of Inflammatory, Apoptotic, Mitochondrial and Damaged Mediators in Spinal Dorsal Horn (SDH) by Day 30 After CCI (Fig. 5)

The protein expressions of TNF-α, NF-κB, IL-1ß and MMP-9, four indicators of inflammation, were highest in CCI, lowest in SC, significantly higher in CCI + ECSW and CCI + Mel than in CCI + ECSW + Mel, and significantly higher in CCI + Mel than in CCI + ECSW. Additionally, the protein expressions of mitochondrial Bax, cleaved caspase 3 and cleaved PARP, three apoptotic biomarkers, revealed an identical pattern of inflammation among the five groups. Furthermore, the protein expressions of γ-H2AX, an indicator of DNA damage, exhibited an identical pattern to apoptosis among the five groups. Moreover, protein expression of cytosolic cytochrome C, an indicator of mitochondrial-damage, displayed an identical pattern of γ-H2AX among the five groups.

Protein Expressions of Oxidative Stress Biomarkers, Signaling Transduction Molecules, Microglia and Astrocyte Activity in SDH by Day 30 After CCI (Fig. 6)

The protein expressions of NOX-1, NOX-2, NOX-4 and oxidized protein, four indicators of oxidative stress, were highest in CCI, lowest in SC, significantly higher in CCI + ECSW and CCI + Mel than in CCI + ECSW + Mel, and significantly higher in CCI + Mel than in CCI + ECSW. Additionally, the

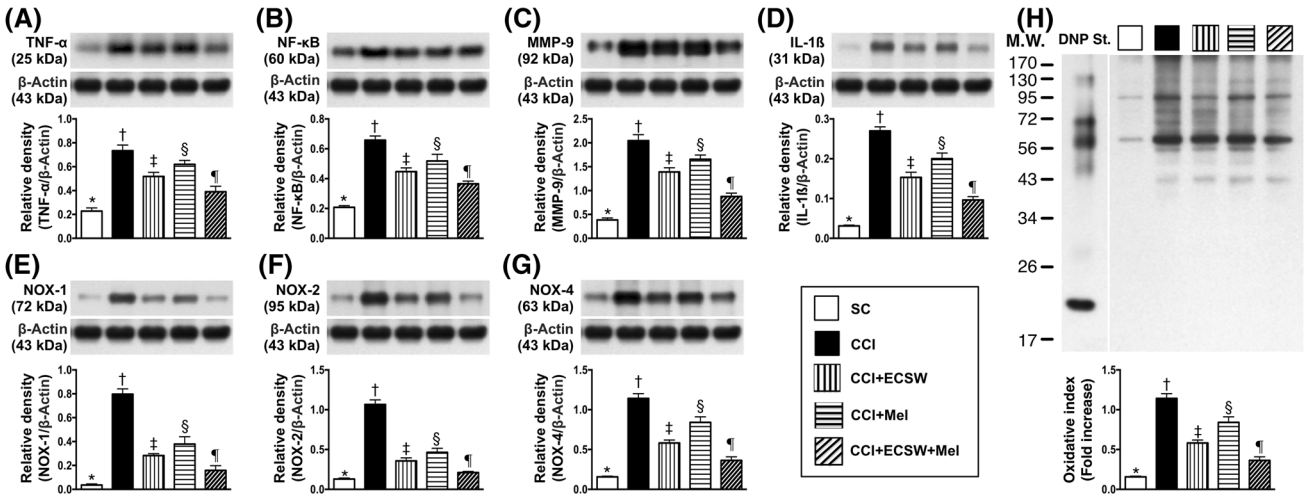

Fig. 3 The protein expressions of inflammatory and oxidative stress biomarkers in L4-5 DRGs by day 30 after CCI. **a** Protein expression of tumor necrosis factor (TNF)-α, * denotes statistical significance versus other groups with different symbols (†, ‡, §, ¶), $p < 0.0001$. **b** Protein expression of nuclear factor (NF)-κB, * denotes statistical significance versus other groups with different symbols (†, ‡, §, ¶), $p < 0.0001$. **c** Protein expression of matrix metalloproteinase (MMP)-9, * denotes statistical significance versus other groups with different symbols (†, ‡, §, ¶), $p < 0.0001$. **d** Protein expression of interleukin (IL)-1ß, * denotes statistical significance versus other groups with different symbols (†, ‡, §, ¶), $p < 0.0001$. **e** Protein expression of NOX-1, * denotes statistical significance versus other groups with different symbols (†, ‡, §, ¶), $p < 0.0001$. **f** Protein expression of NOX-2, * denotes statistical significance versus other groups with different symbols (†, ‡, §, ¶), $p < 0.0001$. **g** Protein expression of NOX-4, * denotes statistical significance versus other groups with different symbols (†, ‡, §, ¶), $p < 0.0001$. Group 4 than in group 3. **h** Oxidized protein expression, * versus other groups with different symbols (†, ‡, §, ¶), $p < 0.0001$. (Note: left lanes shown on the upper panel represent protein molecular weight marker and control oxidized molecular protein standard, respectively). *MW* molecular weight, *DNP* 1–3 dinitrophenylhydrazone. All statistical analyses were performed by one-way ANOVA, followed by Bonferroni multiple comparison post hoc test ($n = 6$ for each group). Symbols (*, †, ‡, §, ¶) indicate significance at the 0.05 level (i.e., SC vs. CCI, $p < 0.0001$; CCI vs. CCI + ECSW vs. CCI + Mel vs. CCI + ECSW + Mel, $p < 0.0001$; CCI + ECSW + Mel vs. CCI + ECSW, $p < 0.01$; CCI + ECSW + Mel vs. CCI + Mel, $p < 0.001$; CCI + ECSW vs. CCI + Mel, $p < 0.05$). *SC* sham control, *CCI* chronic constriction injury, *ECSW* extracorporeal shock wave, *Mel* melatonin

protein expressions of p-p38, p-JNK, p-ERK1/2, three indicators of MAPKs, exhibited an identical pattern to oxidative stress among the five group. Furthermore, the neuroinflammatory protein expressions of ox42, an indicator of microglia activation, and GFAP, an indicator of astrocyte activation, displayed an identical pattern to MAPKs among the five groups.

IF Microscopy for Co-localizations of p-ERK/ p-JNK and Peripherin in L4-5 DRG Neurons by Day 30 After CCI (Fig. 7)

To clarify the activation of MAPKs, the expression of p-ERK/p-JNK activations were measured. IF microscopy identified that the expressions of p-ERK (upper panel) and p-JNK (lower panel) in peripherin, two indicators of MAPKs activation in small unmyelinated C-fiber and thinly myelinated A-δ fiber of DRG neurons that transmit signals of thermal and noxious stimuli, were lowest in SC, highest in CCI, significantly higher in CCI + ECSW and CCI + Mel than in CCI + ECSW + Mel, and significantly higher in CCI + Mel than in CCI + ECSW.

IF Microscopy for Co-localizations of p-ERK/ p-JNK and NF200 in L4-5 DRG Neurons by Day 30 After CCI (Fig. 8)

IF microscopy identified that p-ERK (upper panel) and p-JNK (lower panel) expressions in NF200, two indicators of MAPKs activation in large myelinated A-β fiber of DRG neurons that transmit information of non-noxious mechanical stimuli as well as abnormal mechanical allodynia in the pathologic neuropathic pain, were lowest in SC, highest in CCI, significantly higher in CCI + ECSW and CCI + Mel than in CCI + ECSW + Mel, and significantly higher in CCI + Mel than in CCI + ECSW.

IF Microscopy for Co-localizations of Nav1.8/ Nav1.9 and Peripherin in L4-5 DRG Neurons by Day 30 After CCI (Fig. 9)

IF microscopy identified that Nav1.8 (upper panel) and Nav1.9 (lower panel) expressions in peripherin, two indicators of voltage-gated sodium channels in small unmyelinated C-fiber and thinly myelinated A-δ fiber of DRG neurons that transmit signals of thermal and

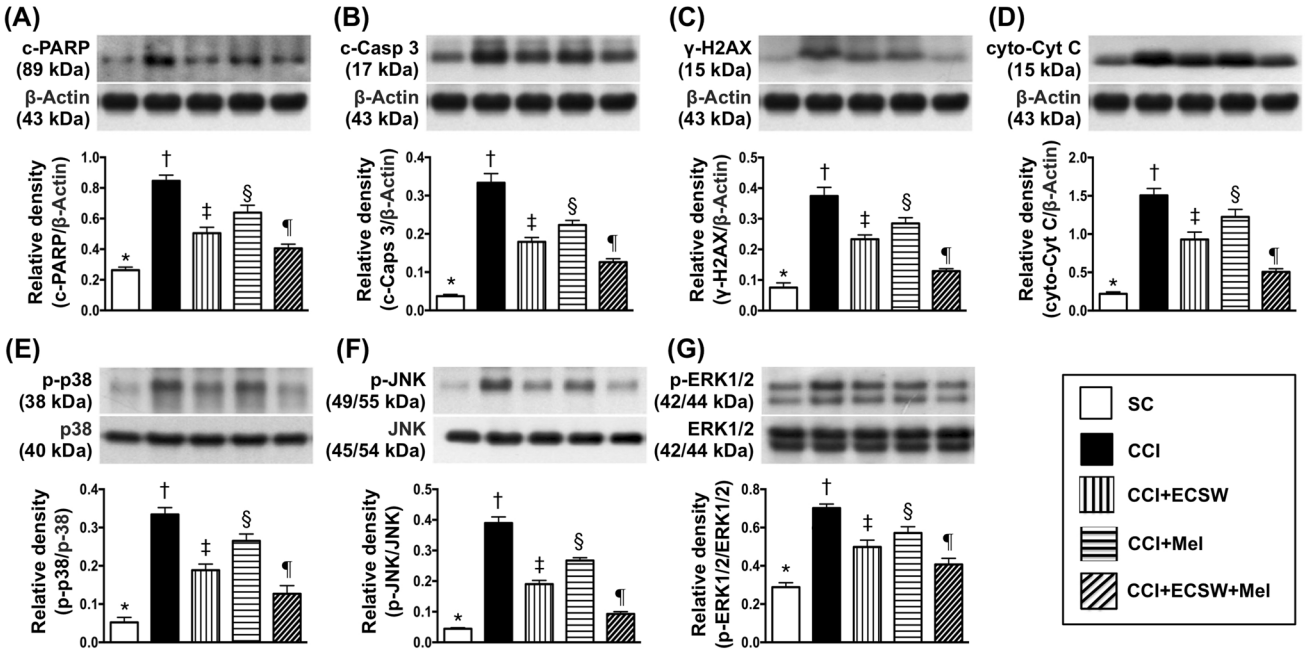

Fig. 4 Protein expressions of apoptotic, mitochondrial-damaged and DNA damaged biomarkers, and signaling transduction molecules in L4-5 DRGs by day 30 after CCI. **a** Protein expression of cleaved poly (ADP-ribose) polymerase (c-PARP), * denotes statistical significance versus other groups with different symbols (†, ‡, §, ¶), $p < 0.0001$. **b** Protein expression of cleaved caspase (c-Casp) 3, * denotes statistical significance versus other groups with different symbols (†, ‡, §, ¶), $p < 0.0001$. **c** Protein expression of γ-H2AX, * denotes statistical significance versus other groups with different symbols (†, ‡, §, ¶), $p < 0.0001$. **d** Protein expression of cytosolic cytochrome C (cyto-Cyt C), * denotes statistical significance versus other groups with different symbols (†, ‡, §, ¶), $p < 0.0001$. **e** Protein expression of phosphorylated (p)-p38, * denotes statistical significance versus other groups with different symbols (†, ‡, §, ¶), $p < 0.0001$. **f** Protein expression of p-JNK, * denotes statistical significance versus other groups with different symbols (†, ‡, §, ¶), $p < 0.001$. **g** Protein expression of p-ERK1/2, * denotes statistical significance versus other groups with different symbols (†, ‡, §, ¶), $p < 0.0001$. All statistical analyses were performed by one-way ANOVA, followed by Bonferroni multiple comparison post hoc test ($n = 6$ for each group). Symbols (*, †, ‡, §, ¶) indicate significance at the 0.05 level (i.e., SC vs. CCI, $p < 0.0001$; CCI vs. CCI + ECSW vs. CCI + Mel vs. CCI + ECSW + Mel, $p < 0.0001$; CCI + ECSW + Mel vs. CCI + ECSW, $p < 0.01$; CCI + ECSW + Mel vs. CCI + Mel, $p < 0.001$; CCI + ECSW vs. CCI + Mel, $p < 0.05$). *SC* sham control, *CCI* chronic constriction injury, *ECSW* extracorporeal shock wave, *Mel* melatonin

noxious stimuli, were lowest in SC, highest in CCI, significantly higher in CCI + ECSW and CCI + Mel than in CCI + ECSW + Mel, and significantly higher in CCI + Mel than in CCI + ECSW.

IF microscopy for co-localizations of Nav1.8/Nav1.9 and NF200 in L4-5 DRG neurons by day 30 after CCI (Fig. 10)

IF microscopy identified that Nav1.8 (upper panel) and Nav1.9 (lower panel) expressions in NF200, two indicators of voltage-gated sodium channels in large myelinated A-β fiber of DRG neurons that transmit information of non-noxious mechanical stimuli as well as abnormal mechanical allodynia in the pathologic neuropathic pain, was lowest in SC, highest in CCI, significantly higher in CCI + ECSW and CCI + Mel than in CCI + ECSW + Mel, and significantly higher in CCI + Mel than in CCI + ECSW.

Discussion

This study which investigated the therapeutic impact of ECSW-supported Mel on improving NP yielded several striking preclinical implications. Frist, inflammatory reaction and oxidative stress were markedly increased in DRG and SDH as well as microglia and astrocyte activities were substantially activated in SDH, suggesting that molecular perturbations were elicited in NP. Second, abundant parameters involved in the transmission of painful sensation were identified to be markedly enhanced not only in DRG/SDH but also in sciatic nerve, suggesting that a rather complicated signaling pathway participated in induction of NP that would, therefore, be expected that monotherapy would be commonly ineffective in inhibiting NP, especially when a long-term effect to be taken into consideration. Third, combined therapy with ECSWM-Mel was identified to offer a synergistic effect for suppressing the NP (including mechanical allodynia and thermal hyperalgesia), highlighting that this combination regimen may possess a therapeutic

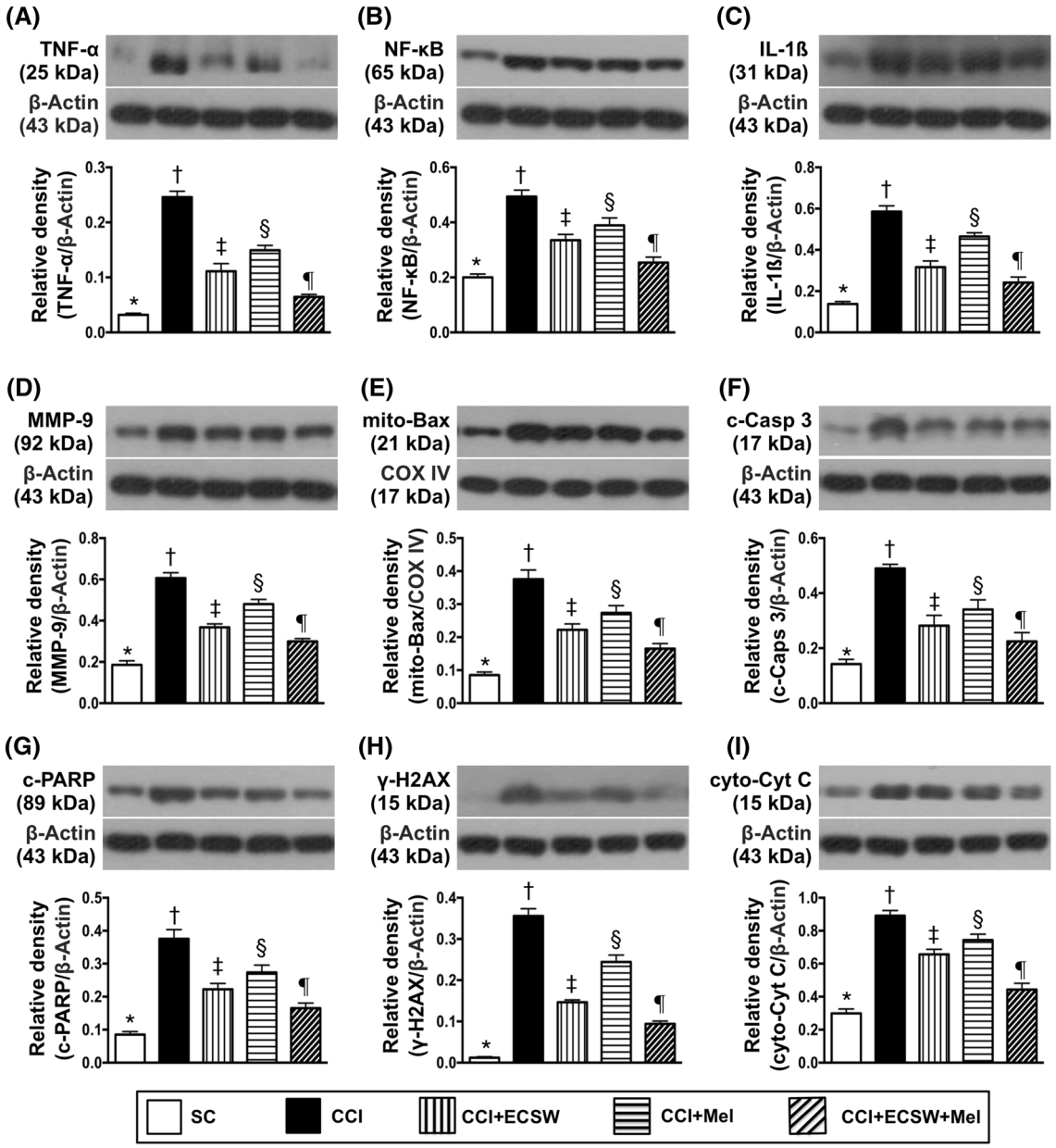

Fig. 5 Protein expressions of inflammatory, apoptotic, mitochondrial and damaged mediators in spinal dorsal horn (SDH) by day 30 after CCI. **a** Protein expression of tumor necrosis factor (TNF)-α, * denotes statistical significance versus other groups with different symbols (†, ‡, §, ¶), $p < 0.0001$. **b** Protein expression of nuclear factor (NF)-κB, * denotes statistical significance versus other groups with different symbols (†, ‡, §, ¶), $p < 0.001$. **c** Protein expression of interleukin (IL)-1ß, * denotes statistical significance versus other groups with different symbols (†, ‡, §, ¶), $p < 0.0001$. **d** Protein expression of matrix metalloproteinase (MMP)-9, * denotes statistical significance versus other groups with different symbols (†, ‡, §, ¶), $p < 0.0001$. **e** Protein expressions of mitochondrial (Mito)-Bax, * denotes statistical significance versus other groups with different symbols (†, ‡, §, ¶), $p < 0.001$. **f** Protein expression of cleaved poly (ADP-ribose) polymerase (c-PARP), * denotes statistical significance versus other groups with different symbols (†, ‡, §, ¶), $p < 0.0001$. **g** Protein expressions of γ-H2AX, * denotes statistical significance versus other groups with different symbols (†, ‡, §, ¶), $p < 0.001$. All statistical analyses were performed by one-way ANOVA, followed by Bonferroni multiple comparison post hoc test ($n = 6$ for each group). Symbols (*, †, ‡, §, ¶) indicate significance at the 0.05 level (i.e., SC vs. CCI, $p < 0.0001$; CCI vs. CCI + ECSW vs. CCI + Mel vs. CCI + ECSW + Mel, $p < 0.0001$; CCI + ECSW + Mel vs. CCI + ECSW, $p < 0.01$; CCI + ECSW + Mel vs. CCI + Mel, $p < 0.001$; CCI + ECSW vs. CCI + Mel, $p < 0.05$). *SC* sham control, *CCI* chronic constriction injury, *ECSW* extracorporeal shock wave, *Mel* melatonin

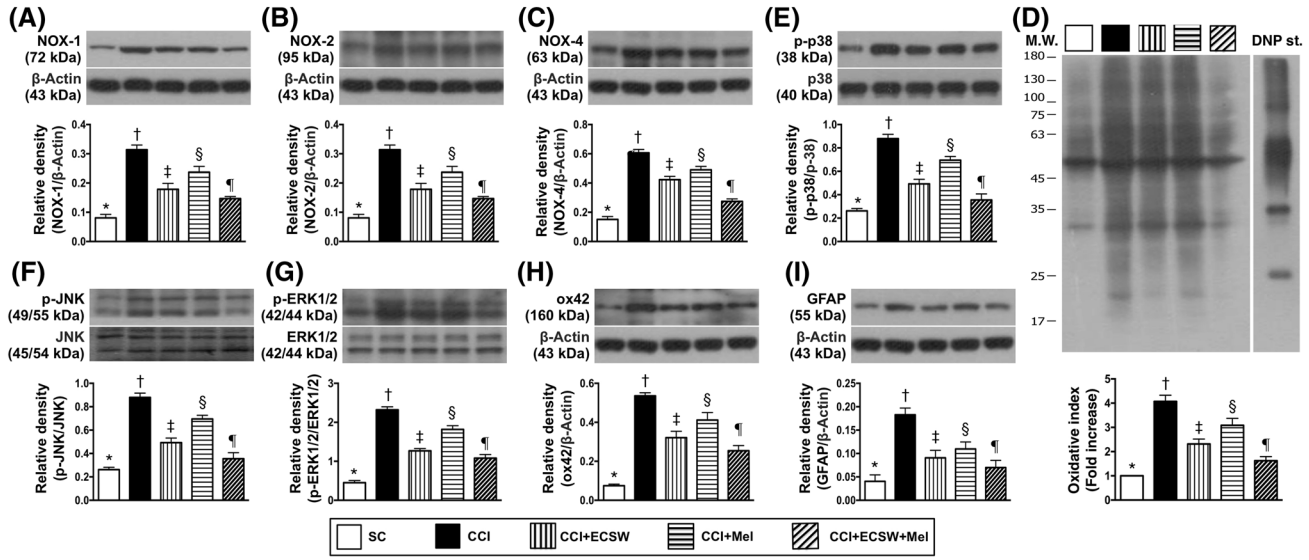

Fig. 6 Protein expressions of oxidative stress biomarkers, signaling transduction molecules, microglia and astrocyte activity in SDH by day 30 after CCI. **a** The protein expression of NOX-1, * denotes statistical significance versus other groups with different symbols (†, ‡, §, ¶), $p<0.0001$. **b** Protein expression of NOX-2, * denotes statistical significance versus other groups with different symbols (†, ‡, §, ¶), $p<0.0001$. **c** Protein expression of NOX-4, * denotes statistical significance versus other groups with different symbols (†, ‡, §, ¶), $p<0.0001$. **d** Oxidized protein expression, * versus other groups with different symbols (†, ‡, §, ¶), $p<0.0001$. (Note: left lanes shown on the upper panel represent protein molecular weight marker and control oxidized molecular protein standard, respectively). M.W = molecular weight; DNP = 1–3 dinitrophenylhydrazone. **e** Protein expressions of phosphorylated (p)-p38, * denotes statistical significance versus other groups with different symbols (†, ‡, §, ¶), $p<0.0001$. **f** Protein expression of p-JNK, * denotes statistical significance versus other groups with different symbols (†, ‡, §, ¶), $p<0.0001$. **g** Protein expression of p-ERK1/2, * denotes statistical significance versus other groups with different symbols (†, ‡, §, ¶), $p<0.0001$. **h** Neuroinflammatory protein expressions of ox42, * denotes statistical significance versus other groups with different symbols (†, ‡, §, ¶), $p<0.0001$. **i** Protein expression of Glial Fibrillary Acidic Protein (GFAP), * denotes statistical significance versus other groups with different symbols (†, ‡, §, ¶), $p<0.0001$. All statistical analyses were performed by one-way ANOVA, followed by Bonferroni multiple comparison post hoc test ($n=6$ for each group). Symbols (*, †, ‡, §, ¶) indicate significance at the 0.05 level (i.e., SC vs. CCI, $p<0.0001$; CCI vs. CCI + ECSW vs. CCI + Mel vs. CCI + ECSW + Mel, $p<0.0001$; CCI + ECSW + Mel vs. CCI + ECSW, $p<0.01$; CCI + ECSW + Mel vs. CCI + Mel, $p<0.001$; CCI + ECSW vs. CCI + Mel, $p<0.05$). *SC* sham control, *CCI* chronic constriction injury, *ECSW* extracorporeal shock wave, *Mel* melatonin

potential for NP patients, especially when conventional therapy is ineffective for those of NP patients.

Undoubtedly, the treatment of NP is still a formidable challenge for physicians [6, 7]. One important finding in the present study was that as compared with NP animals, MPWT and TPWL were significantly increased by ECSW and Mel therapy. The most important finding in the present study was that ECSW-assisted Mel therapy was superior to either one alone for attenuating mechanical allodynia and thermal hyperalgesia, highlighting that combined ECSW-Mel therapy may be an innovative therapy for those of NP patients who are refractory to conventional one.

Although our recent study [1] has shown that ECSW-Mel therapy effectively alleviated the mechanical allodynia and thermal hyperalgesia of NP in rodent, the study period was too short (i.e., the study period was only 8 days) and did not provide adequate information regarding the long-term effect of ECSW-Mel therapy on NP. Accordingly, we performed the present study to answer the question left by our recent study [1]. Interestingly, the results of the present study demonstrated that the therapeutic effect on suppressing mechanical allodynia (i.e., increasing MPWT) was persistently similar between ECSW and Mel (i.e., by time points of days 15, 22, 29). In this way, the result of our present study was consistent with the finding of our recent report [1]. Another interesting finding in the present study was that when we looked at the alternation of TPWL, we found that the TPWL was persistently and significantly higher in Mel-treated NP animals than in ECSW-treated NP animals at time points of days 15, 22 and 29 after CCI procedure that were not found in our recent study [1] at time points of days 2 and 8 after CCI procedure. In this way, the findings of the present study extended the findings of our recent study [1].

Plentiful data have shown that both inflammatory reaction and oxidative stress are always increased in damaged/ischemic tissues and organs [10, 22, 23]. Additionally, link between NP and upregulation of inflammation and oxidative stress has been keenly investigated by recent studies [1–3, 5]. Another important finding in the present study was that as compared with SC animals, the inflammatory

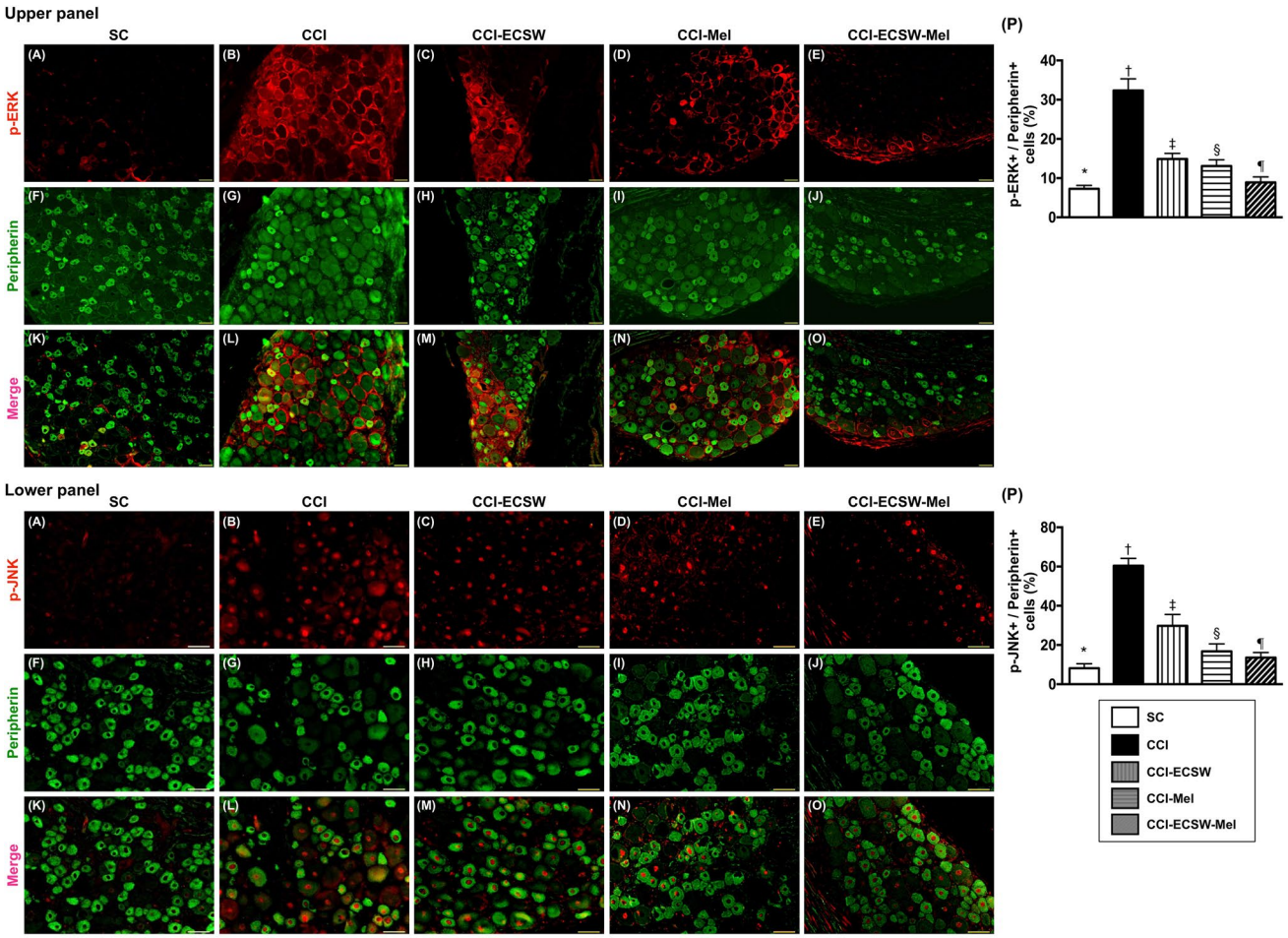

Fig. 7 Immunofluorescent (IF) microscopic finding for co-localizations of p-ERK/ p-JNK and peripherin in L4-5 DRG neurons by day 30 after CCI. Upper: **a–e** Illustrating the IF microscopic finding (× 200) positively stained phosphorylated (p)-ERK cells in DRG neurons (red color). **f** to **j** Illustrating the IF microscopic finding (× 200) positively stained peripherin cells (green color). **k** to **o** Illustrating the IF microscopic finding (× 200) of merged positively-stained p-ERK and peripherin (green–red colocalization). **p** Statistical results of number of p-ERK+/peripherin + cells, * denotes statistical significance versus other groups with different symbols (†, ‡, §, ¶), $p < 0.0001$. Lower: **a–e** Illustrating the IF microscopic finding (× 200) positively stained phosphorylated (p)-JNK cells in DRG neurons (red color). **f** to **j** Illustrating the IF microscopic finding (× 200) positively stained peripherin cells (green color). **k–o** Illustrating the IF microscopic finding (× 200) of merged positively-stained p-JNK and peripherin (green–red colocalization). **p** Statistical results of number of p-JNK+/peripherin + cells, * denotes statistical significance versus other groups with different symbols (†, ‡, §, ¶), $p < 0.0001$. The scale bars in right lower corner represent 50 μm. All statistical analyses were performed by one-way ANOVA, followed by Bonferroni multiple comparison post hoc test ($n = 6$ for each group). Symbols (*, †, ‡, §, ¶) indicate significance at the 0.05 level (i.e., SC vs. CCI, $p < 0.0001$; CCI vs. CCI + ECSW vs. CCI + Mel vs. CCI + ECSW + Mel, $p < 0.0001$; CCI + ECSW + Mel vs. CCI + ECSW, $p < 0.01$; CCI + ECSW + Mel vs. CCI + Mel, $p < 0.001$; CCI + ECSW vs. CCI + Mel, $p < 0.05$). *SC* sham control, *CCI* chronic constriction injury, *ECSW* extracorporeal shock wave, *Mel* melatonin

reaction and oxidative stress as well as those of CNS-specific inflammatory/immune cells (i.e., microglias and astrocytes) were remarkably enhanced and activated in NP animals. Importantly, these parameters in NP animals were notably suppressed by either ECSMW or Mel therapy and further notably suppressed by combined ECSW-Mel therapy. Accordingly, our findings, in addition to reinforcing the findings of recent studies [1–3, 5], could, at least in part, explain for why ECSW-Mel therapy attenuated mechanical allodynia and thermal hyperalgesia in NP animals.

It is well recognized that the MAPK signal pathways activation (i.e., p-p38, p-JNK, p-ERK1/2) plays intrinsically crucial role in response to stress stimulations/painful transduction and maintenance in DRGs and SDH, especially when these nervous systems are damaged [1, 16, 24, 25]. Additionally, voltage-gated sodium channels (i.e., Nav.1.3, Nav.1.8 and Nav.1.9) have been also clearly elucidated to play essential roles for sensitization of pain-conduction pathways of the peripheral nervous system [1, 17]. The essential findings in the present study were that these parameters

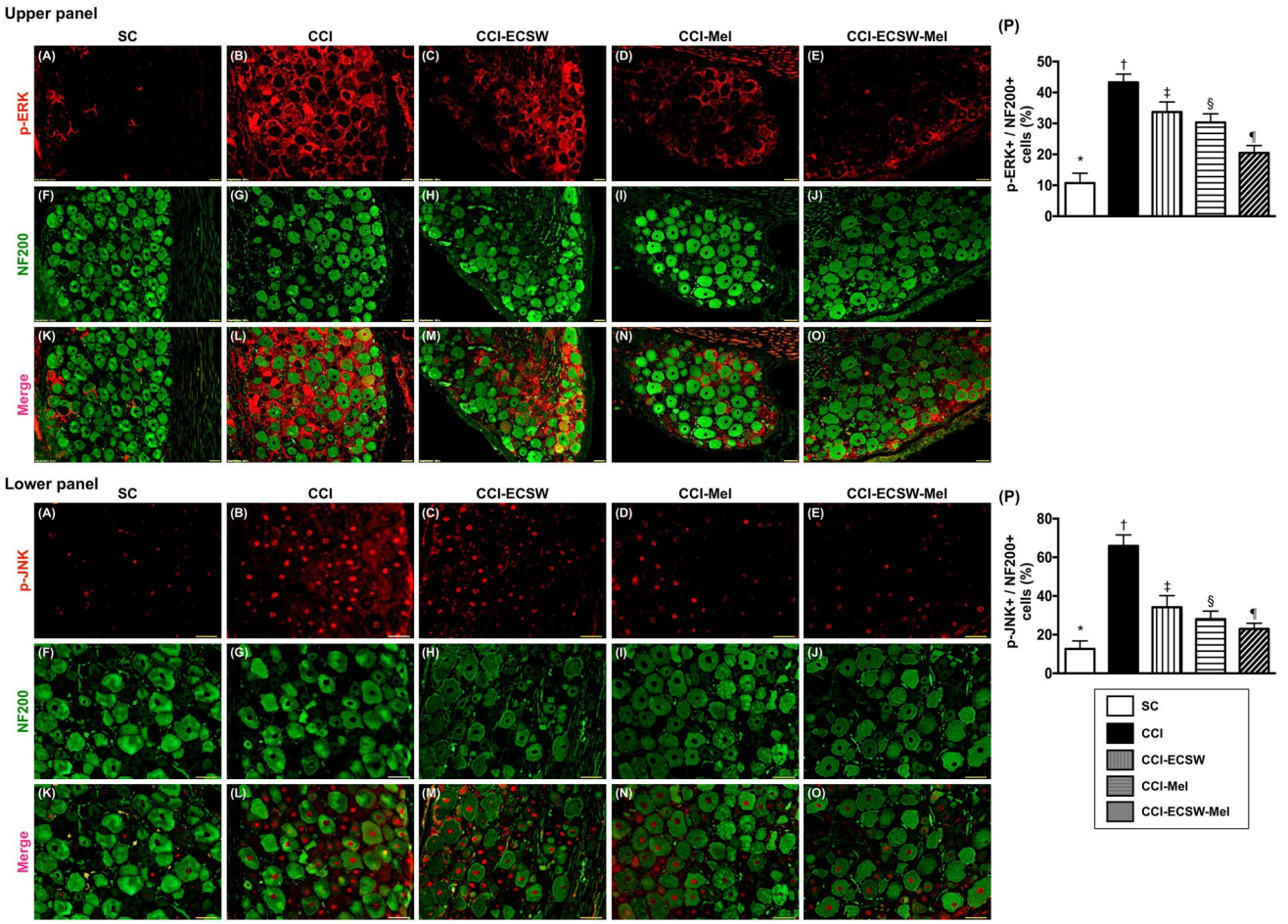

Fig. 8 Immunofluorescent (IF) microscopic finding for co-localizations of p-ERK/ p-JNK and NF200 in L4-5 DRG neurons by day 30 after CCI. Upper: **a**–**e** Illustrating the IF microscopic finding (× 200) positively stained phosphorylated (p)-ERK cells in DRG neurons (red color). **f**–**j** Illustrating the IF microscopic finding (× 200) positively stained NF200 cells (green color). **k**–**o** Illustrating the IF microscopic finding (× 200) of merged positively-stained p-ERK and NF200 (green–red colocalization). **p** Statistical results of number of p-ERK+/NF200 + cells, * denotes statistical significance versus other groups with different symbols (†, ‡, §, ¶), $p < 0.0001$. Lower Lower: **a**–**e** Illustrating the IF microscopic finding (× 200) positively stained p-JNK cells in DRG neurons (red color spots). **f**–**j** Illustrating the IF microscopic finding (× 200) positively stained NF200 cells (green color). **k**–**o** Illustrating the IF microscopic finding (× 200) of merged positively-stained p-JNK and NF200 (green–red colocalization). **p** Statistical results of number of p-JNK+/NF200 + cells, * denotes statistical significance versus other groups with different symbols (†, ‡, §, ¶), $p < 0.0001$. The scale bars in right lower corner represent 50 µm. All statistical analyses were performed by one-way ANOVA, followed by Bonferroni multiple comparison post hoc test ($n = 6$ for each group). Symbols (*, †, ‡, §, ¶) indicate significance at the 0.05 level (i.e., SC vs. CCI, $p < 0.0001$; CCI vs. CCI + ECSW vs. CCI + Mel vs. CCI + ECSW + Mel, $p < 0.0001$; CCI + ECSW + Mel vs. CCI + ECSW, $p < 0.01$; CCI + ECSW + Mel vs. CCI + Mel, $p < 0.001$; CCI + ECSW vs. CCI + Mel, $p < 0.05$). *SC* sham control, *CCI* chronic constriction injury, *ECSW* extracorporeal shock wave, *Mel* melatonin

were significantly increased in NP animals than in those of SC counterparts. Our findings strengthened the findings of those previous studies [1, 16, 17, 24, 25]. Of importance was that these mediators were remarkably suppressed by Mel therapy, more suppressed by ECSW therapy and furthermore suppressed by combined ECSW-Mel therapy in NP animals. Our findings once again partially explained why the mechanical allodynia and thermal hyperalgesia were markedly ameliorated in NP animals after receiving ECSW-assisted Mel therapy.

Inflammation and oxidative stress commonly elicit the apoptosis and DNA/mitochondrial damages in ischemia-related organ dysfunction [10, 22, 23]. A principal finding in the present study was that those aforementioned parameters were notably increased in NP than in SC animals. Our finding was consistent with the findings of previous studies [1, 10, 22]. Of distinctive finding in the present study was that these molecular perturbations were remarkably inhibited in NP animals after receiving ECSW-Mel combined therapy, which might be reflected by

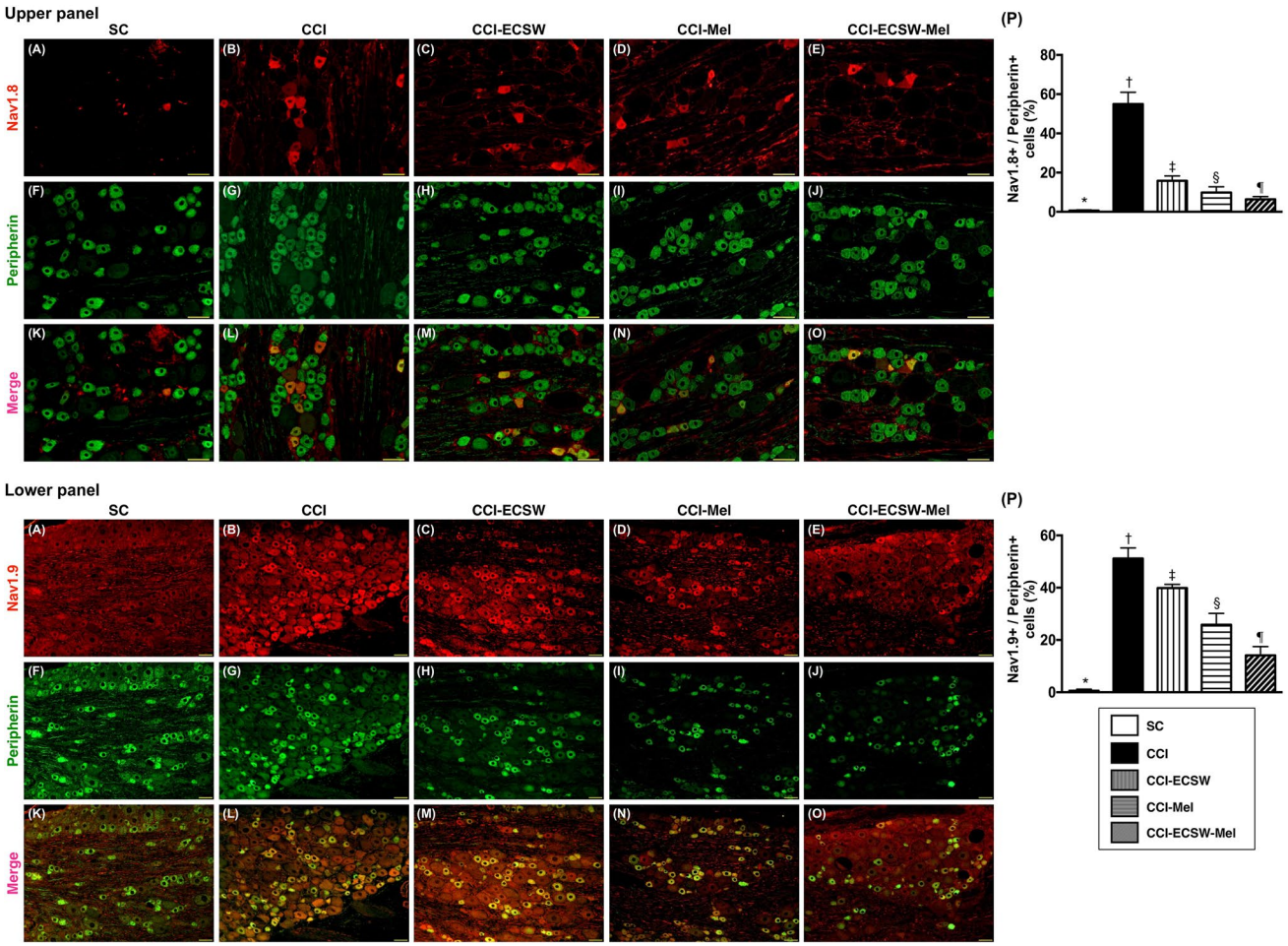

Fig. 9 Immunofluorescent (IF) microscopic finding for co-localizations of Nav1.8/ Nav1.9 and peripherin in L4-5 DRG neurons by day 30 after CCI. Upper panel: **a–e** Illustrating the IF microscopic finding (× 200) positively stained Nav1.8 cells in DRG neurons (red color). **f–j** Illustrating the IF microscopic finding (× 200) positively stained peripherin cells (green color). **k–o** Illustrating the IF microscopic finding (× 200) of merged positively-stained Nav1.8 and peripherin (green–red colocalization). **p** Statistical results of number of Nav1.8+/peripherin + cells, * denotes statistical significance versus other groups with different symbols (†, ‡, §, ¶), $p < 0.0001$. Lower: **a–e** Illustrating the IF microscopic finding (× 200) positively stained Nav1.9 cells in DRG neurons (red color). **f–j** Illustrating the IF microscopic finding (× 200) positively stained peripherin cells (green color). **k–o** Illustrating the IF microscopic finding (× 200) of merged positively-stained Nav1.9 and peripherin (green–red colocalization). **p** Statistical results of number of Nav1.9+/peripherin + cells, * denotes statistical significance versus other groups with different symbols (†, ‡, §, ¶), $p < 0.0001$. The scale bars in right lower corner represent 50 µm. All statistical analyses were performed by one-way ANOVA, followed by Bonferroni multiple comparison post hoc test ($n = 6$ for each group). Symbols (*, †, ‡, §, ¶) indicate significance at the 0.05 level (i.e., SC vs. CCI, $p < 0.0001$; CCI vs. CCI + ECSW vs. CCI + Mel vs. CCI + ECSW + Mel, $p < 0.0001$; CCI + ECSW + Mel vs. CCI + ECSW, $p < 0.01$; CCI + ECSW + Mel vs. CCI + Mel, $p < 0.001$; CCI + ECSW vs. CCI + Mel, $p < 0.05$). *SC* sham control, *CCI* chronic constriction injury, *ECSW* extracorporeal shock wave, *Mel* melatonin

improvement on mechanical allodynia and thermal hyperalgesia in CCI-induced NP.

Study Limitations

This study has limitations. First, we did not test the optimal dosage in stepwise increase manner in both ECSW and Mel. Therefore, we did not provide direct evidence for supporting ECSW therapy is superior to Mel for suppressing the NP or vice versa. Second, this study did not provide long-term effect of ECSW-Mel therapy on attenuating the NP in rodent, such as more than 6-month follow up, because this is out of study scope. Third, we did not offer the underlying mechanism(s) of action(s) of the investigated therapies responsible for suppressing all those molecules perturbations, because of the extreme complexity of NP.

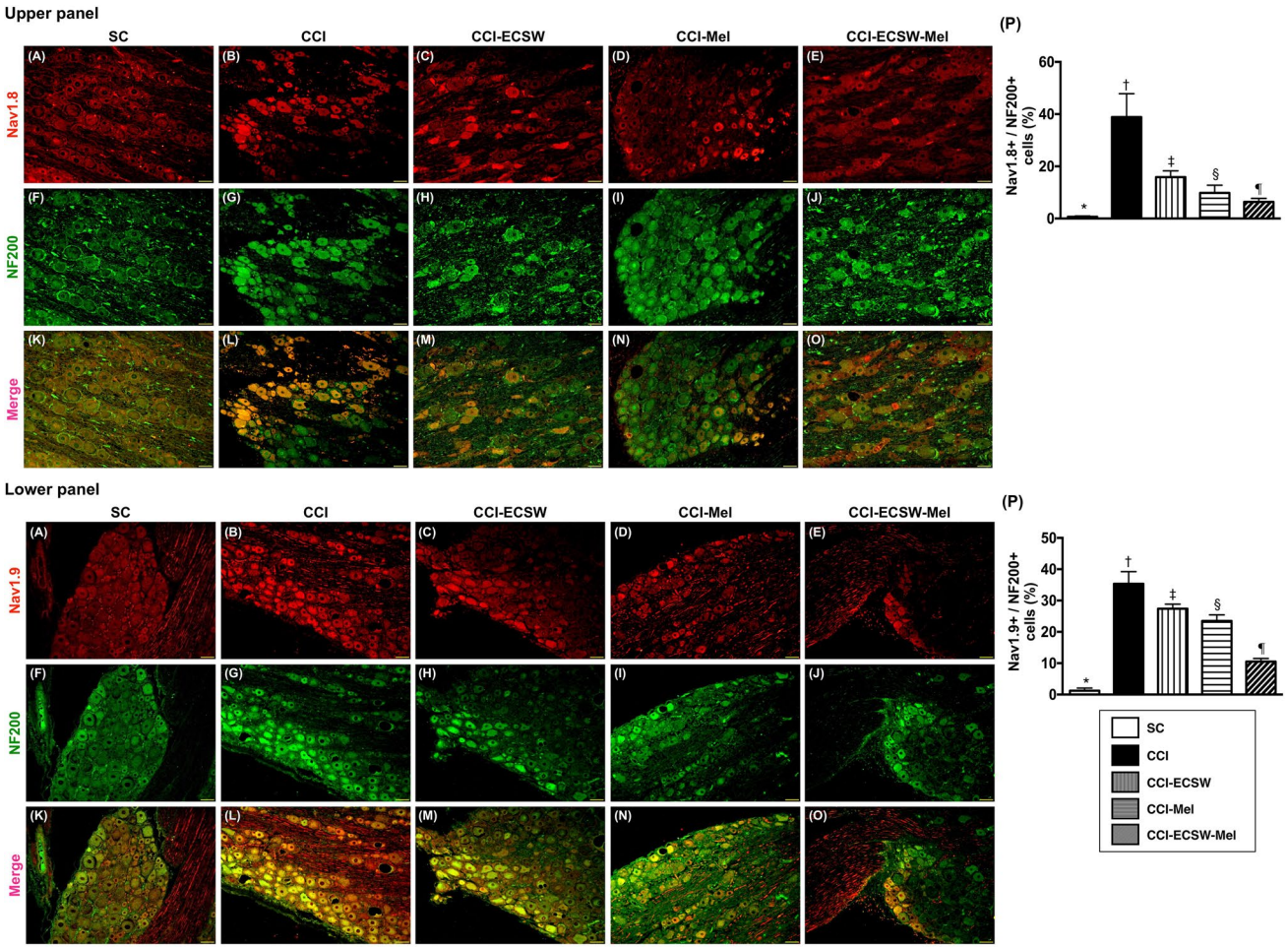

Fig. 10 Immunofluorescent (IF) microscopic finding for co-localizations of Nav1.8/Nav1.9 and NF200 in L4-5 DRG neurons by day 30 after CCI. Upper: **a**–**e** Illustrating the IF microscopic finding (× 200) positively stained Nav1.8 cells in DRG neurons (red color). **f**–**j** Illustrating the IF microscopic finding (× 200) positively stained NF200 cells (green color). **k**–**o** Illustrating the IF microscopic finding (× 200) of merged positively-stained Nav1.8 and NF200 (green–red colocalization). **p** Statistical results of number of Nav1.8+/NF200 + cells, * denotes statistical significance versus other groups with different symbols (†, ‡, §, ¶), $p < 0.0001$. Lower **a**–**e** Illustrating the IF microscopic finding (× 200) positively stained Nav1.9 cells in DRG neurons (red color). **f**–**j** Illustrating the IF microscopic finding (× 200) positively stained NF200 cells (green color). **k**–**o** Illustrating the IF microscopic finding (× 200) of merged positively-stained Nav1.9 and NF200 (green–red colocalization). **p** Statistical results of number of Nav1.9+/NF200 + cells, * denotes statistical significance versus other groups with different symbols (†, ‡, §, ¶), $p < 0.0001$. The scale bars in right lower corner represent 50 μm. All statistical analyses were performed by one-way ANOVA, followed by Bonferroni multiple comparison post hoc test ($n = 6$ for each group). Symbols (*, †, ‡, §, ¶) indicate significance at the 0.05 level (i.e., SC vs. CCI, $p < 0.0001$; CCI vs. CCI + ECSW vs. CCI + Mel vs. CCI + ECSW + Mel, $p < 0.0001$; CCI + ECSW + Mel vs. CCI + ECSW, $p < 0.01$; CCI + ECSW + Mel vs. CCI + Mel, $p < 0.001$; CCI + ECSW vs. CCI + Mel, $p < 0.05$). *SC* sham control, *CCI* chronic constriction injury, ECSW extracorporeal shock wave, *Mel* melatonin

Conclusion

In conclusion, the synergistic effect of combined ECSW-Mel therapy is superior to either one alone for long-term improvement of mononeuropathic pain-induced by CCI in rats.

Acknowledgements This study was supported by a program grant from Chang Gung Memorial Hospital, Chang Gung University (Grant Nos.: CMRPG8E0771, CMRPG8E1361).

Author Contributions H-KY, C-HY and K-HC conceived of the study, and participated in the design of the study, data acquisition and analysis as well as drafting the manuscript. H-FC edited the manuscript. T-CY, JYC, P-H, K-CL and Y-LC were responsible for the laboratory assay and troubleshooting., Y-C, Ti-H, C-RH and CL participated in data acquisition, analysis, and interpretation. All authors read and approved the final manuscript.

Compliance with Ethical Standards

Conflict of interest The authors declare that they have no conflicts of interest.

References

1. Chen KH, Yang CH, Wallace CG, Lin CR, Liu CK, Yin TC, Huang TH, Chen YL, Sun CK, Yip HK (2017) Combination therapy with extracorporeal shock wave and melatonin markedly attenuated neuropathic pain in rat. Am J Transl Res 9(10):4593–4606
2. Chen YL, Chen KH, Yin TC, Huang TH, Yuen CM, Chung SY, Sung PH, Tong MS, Chen CH, Chang HW, Lin KC, Ko SF, Yip HK (2015) Extracorporeal shock wave therapy effectively prevented diabetic neuropathy. Am J Transl Res 7(12):2543–2560
3. Scholz J, Woolf CJ (2007) The neuropathic pain triad: neurons, immune cells and glia. Nat Neurosci 10(11):1361–1368
4. Jensen TS (2002) An improved understanding of neuropathic pain. Eur J Pain 6(Suppl B):3–11
5. Valsecchi AE, Franchi S, Panerai AE, Rossi A, Sacerdote P, Colleoni M (2011) The soy isoflavone genistein reverses oxidative and inflammatory state, neuropathic pain, neurotrophic and vasculature deficits in diabetes mouse model. Eur J Pharmacol 650(2–3):694–702
6. Xu B, Descalzi G, Ye HR, Zhuo M, Wang YW (2012) Translational investigation and treatment of neuropathic pain. Mol Pain 8:15
7. Jensen TS (2002) Anticonvulsants in neuropathic pain: rationale and clinical evidence. Eur J Pain 6(Suppl A):61–68
8. Tan DX, Manchester LC, Hardeland R, Lopez-Burillo S, Mayo JC, Sainz RM, Reiter RJ (2003) Melatonin: a hormone, a tissue factor, an autocoid, a paracoid, and an antioxidant vitamin. J Pineal Res 34(1):75–78
9. Ambriz-Tututi M, Granados-Soto V (2007) Oral and spinal melatonin reduces tactile allodynia in rats via activation of MT2 and opioid receptors. Pain 132(3):273–280
10. Yip HK, Yang CC, Chen KH, Huang TH, Chen YL, Zhen YY, Sung PH, Chiang HJ, Sheu JJ, Chang CL, Chen CH, Chang HW, Chen YT (2015) Combined melatonin and exendin-4 therapy preserves renal ultrastructural integrity after ischemia-reperfusion injury in the male rat. J Pineal Res 59(4):434–447
11. Thomas K (2014) Evolution of extracorporeal shockwave lithotripsy (ESWL). BJU Int 114(5):636
12. Wang CJ (2003) An overview of shock wave therapy in musculoskeletal disorders. Chang Gung Med J 26(4):220–232
13. Wang CJ, Ko JY, Chan YS, Weng LH, Hsu SL (2007) Extracorporeal shockwave for chronic patellar tendinopathy. Am J Sports Med 35(6):972–978
14. Wang CJ, Wang FS, Yang KD, Weng LH, Hsu CC, Huang CS, Yang LC (2003) Shock wave therapy induces neovascularization at the tendon-bone junction. A study in rabbits. J Orthop Res 21(6):984–989
15. Fu M, Sun CK, Lin YC, Wang CJ, Wu CJ, Ko SF, Chua S, Sheu JJ, Chiang CH, Shao PL, Leu S, Yip HK (2011) Extracorporeal shock wave therapy reverses ischemia-related left ventricular dysfunction and remodeling: molecular-cellular and functional assessment. PLoS ONE 6(9):e24342
16. Ji RR, Woolf CJ (2001) Neuronal plasticity and signal transduction in nociceptive neurons: implications for the initiation and maintenance of pathological pain. Neurobiol Dis 8(1):1–10
17. Liu M, Wood JN (2011) The roles of sodium channels in nociception: implications for mechanisms of neuropathic pain. Pain Med 12(Suppl 3):93–99
18. Rogers M, Tang L, Madge DJ, Stevens EB (2006) The role of sodium channels in neuropathic pain. Semin Cell Dev Biol 17(5):571–581
19. Amir R, Argoff CE, Bennett GJ, Cummins TR, Durieux ME, Gerner P, Gold MS, Porreca F, Strichartz GR (2006) The role of sodium channels in chronic inflammatory and neuropathic pain. J Pain 7(5 Suppl 3):S1–S29
20. Baker MD, Wood JN (2001) Involvement of Na^+ channels in pain pathways. Trends Pharmacol Sci 22(1):27–31
21. Bennett GJ, Xie YK (1988) A peripheral mononeuropathy in rat that produces disorders of pain sensation like those seen in man. Pain 33(1):87–107
22. Chai HT, Chen KH, Wallace CG, Chen CH, Sung PH, Chen YL, Yuen CM, Shao PL, Sun CK, Chang HW, Wang CJ, Lee MS, Yip HK, Ko SF (2017) Extracorporeal shock wave therapy effectively protects brain against chronic cerebral hypo-perfusion-induced neuropathological changes. Am J Transl Res 9(11):5074–5093
23. Sun CK, Chen CH, Chang CL, Chiang HJ, Sung PH, Chen KH, Chen YL, Chen SY, Kao GS, Chang HW, Lee MS, Yip HK (2017) Melatonin treatment enhances therapeutic effects of exosomes against acute liver ischemia-reperfusion injury. Am J Transl Res 9(4):1543–1560
24. Ji RR, Samad TA, Jin SX, Schmoll R, Woolf CJ (2002) p38 MAPK activation by NGF in primary sensory neurons after inflammation increases TRPV1 levels and maintains heat hyperalgesia. Neuron 36(1):57–68
25. Zhuang ZY, Gerner P, Woolf CJ, Ji RR (2005) ERK is sequentially activated in neurons, microglia, and astrocytes by spinal nerve ligation and contributes to mechanical allodynia in this neuropathic pain model. Pain 114(1–2):149–159

Affiliations

Chien-Hui Yang[1] · Hon-Kan Yip[2,3,4,5,6] · Hung-Fei Chen[7] · Tsung-Cheng Yin[8] · John Y. Chiang[9] · Pei-Hsun Sung[2] · Kun-Chen Lin[1] · Yu-Huan Tsou[1] · Yi-Ling Chen[2] · Yi-Chen Li[2] · Tien-Hung Huang[2] · Chi-Ruei Huang[2] · Chi-Wen Luo[2] · Kuan-Hung Chen[1,4]

[1] Department of Anesthesiology, Kaohsiung Chang Gung Memorial Hospital and Chang Gung University College of Medicine, No. 123, Dapi Rd., Niaosong Dist, Kaohsiung 83301, Taiwan

[2] Division of Cardiology, Department of Internal Medicine, Kaohsiung Chang Gung Memorial Hospital, Chang Gung University College of Medicine, Kaohsiung 83301, Taiwan

[3] Institute for Translational Research in Biomedicine, Kaohsiung Chang Gung Memorial Hospital, Kaohsiung 83301, Taiwan

[4] Center for Shockwave Medicine and Tissue Engineering, Kaohsiung Chang Gung Memorial Hospital, Kaohsiung 83301, Taiwan

[5] Department of Medical Research, China Medical University Hospital, China Medical University, Taichung 40402, Taiwan

[6] Department of Nursing, Asia University, Taichung 41354, Taiwan

[7] Institute of Technological and Vocational Education, National Pingtung University of Science and Technology, Pingtung 91201, Taiwan

[8] Department of Orthopaedic Surgery, Kaohsiung Chang Gung Memorial Hospital, Chang Gung University College of Medicine, Kaohsiung 83301, Taiwan

[9] Department of Computer Science and Engineering, National Sun Yat-Sen University, Kaohsiung, Taiwan